Acta Cryst E CRYSTALLOGRAPHIC COMMUNICATIONS

ISSN 2056-9890

1-{(*E*)-[(2*E*)-3-(4-Methoxyphenyl)-1-phenylprop-2-en-1-ylidene]amino}-3-phenylurea: crystal structure and Hirshfeld surface analysis

Ming Yueh Tan,[a] Karen A. Crouse,[b,c] Thahira B. S. A. Ravoof,[b]‡ Mukesh M. Jotani[d] and Edward R. T. Tiekink[e]*

[a]Department of Physical Science, Faculty of Applied Sciences, Tunku Abdul Rahman University College, 50932 Setapak, Kuala Lumpur, Malaysia, [b]Department of Chemistry, Faculty of Science, Universiti Putra Malaysia, 43400 UPM Serdang, Selangor Darul Ehsan, Malaysia, [c]Department of Chemistry, St. Francis Xavier University, PO Box 5000, Antigonish, NS B2G 2W5, Canada, [d]Department of Physics, Bhavan's Sheth R. A. College of Science, Ahmedabad, Gujarat 380 001, India, and [e]Research Centre for Crystalline Materials, School of Science and Technology, Sunway University, 47500 Bandar Sunway, Selangor Darul Ehsan, Malaysia. *Correspondence e-mail: edwardt@sunway.edu.my

Received 27 September 2017
Accepted 30 September 2017

Edited by W. T. A. Harrison, University of Aberdeen, Scotland

‡ Additional correspondence author, e-mail: thahira@upm.edu.my.

Keywords: crystal structure; urea derivative; hydrogen bonding; Hirshfeld surface analysis.

CCDC reference: 1577439

Supporting information: this article has supporting information at journals.iucr.org/e

The title compound, $C_{23}H_{21}N_3O_2$, is constructed about an almost planar disubstituted aminourea residue (r.m.s. deviation = 0.0201 Å), which features an intramolecular amine-N—H···N(imine) hydrogen bond. In the 'all-*trans*' chain connecting this to the terminal methoxybenzene residue, the conformation about each of the imine and ethylene double bonds is *E*. In the crystal, amide-N—H···O(carbonyl) hydrogen bonds connect centrosymmetrically related molecules into dimeric aggregates, which also incorporate ethylene-C—H···O(amide) interactions. The dimers are linked by amine–phenyl-C—H···π(imine–phenyl) and methoxybenzene-C—H···π(amine–phenyl) interactions to generate a three-dimensional network. The importance of C—H···π interactions in the molecular packing is reflected in the relatively high contributions made by C···H/H···C contacts to the Hirshfeld surface, *i.e.* 31.6%.

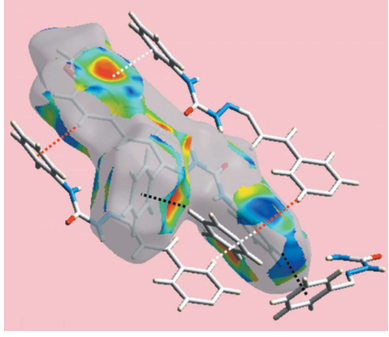

OPEN ACCESS

1. Chemical context

Chalcones are natural or synthetic compounds comprising an open-chain flavonoid structure in which the two aromatic rings are connected *via* a three-carbon-atom α,β-unsaturated carbonyl system. These compounds have attracted much attention due to their diverse pharmacological and biological activities (Gaonkar & Vignesh, 2017), including their anti-cancer (Mahapatra *et al.*, 2015), anti-malarial (Syahri *et al.*, 2017), anti-inflammatory (Li *et al.*, 2017), anti-microbial (Kumar *et al.*, 2017), xanthine oxidase inhibitory (Xie *et al.*, 2017) and aldol reductase inhibitory (Zhuang *et al.*, 2017) properties. The present work is part of an on-going project on the synthesis of chalcone-derived Schiff bases, their ultilization in the synthesis of new transition metal complexes and their investigation as anti-proliferative and anti-bacterial agents. In this context, crystal-structure determinations of a chalcone-derived thiosemicarbazone and a zinc complex have been published (Tan *et al.*, 2015, 2017).

In this contribution, a chalcone residue has been incorporated into a semicarbazide skeleton to form the title chalconesemicarbazone, (I). While chalconesemicarbazone derivatives have shown potential anti-convulsant (Sharma *et al.*, 2014), anti-inflammatory (Singha *et al.*, 2010) and anti-

oxidant activities (Singhal *et al.*, 2011), no crystal structures of chalconesemicarbazone derivatives have been published. Herein, the crystal and molecular structures of (I) have been determined and the study augmented by an analysis of the calculated Hirshfeld surfaces.

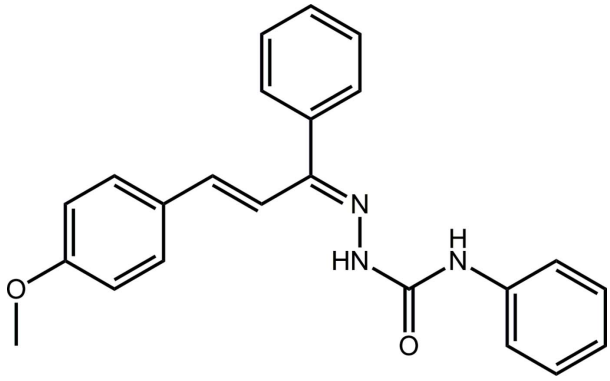

2. Structural commentary

The molecular structure of (I), Fig. 1, comprises a doubly substituted aminourea residue which is close to planar (r.m.s. deviation of CN_3O = 0.0201 Å), owing in part to an intramolecular amine-N—H···N(imine) hydrogen bond, Table 1. The amine-bound phenyl ring is inclined to the CN_3O plane, forming a dihedral angle of 46.88 (4)°. The imine/ethylene sequence of bonds, *i.e.* N3═C8—C9═C10—C11, has an all-*trans* conformation but the N3—C8—C9—C10 and C8—C9—C10—C11 torsion angles of 154.62 (12) and −169.19 (11)°, respectively, indicate some twisting in this residue, especially about the C8—C9 bond; the conformation about each of the double bonds is *E*. The imine-bound phenyl ring forms a dihedral angle of 63.30 (7)° with the C_4N atoms of the imine/ethylene sequence, and the corresponding angle for the terminal methoxybenzene ring is significantly less, at 8.29 (13)°. The methoxy group is twisted out of the plane of the ring to which it is connected as seen in the value of the C17—O18—C14—C15 torsion angle of 15.55 (17)°.

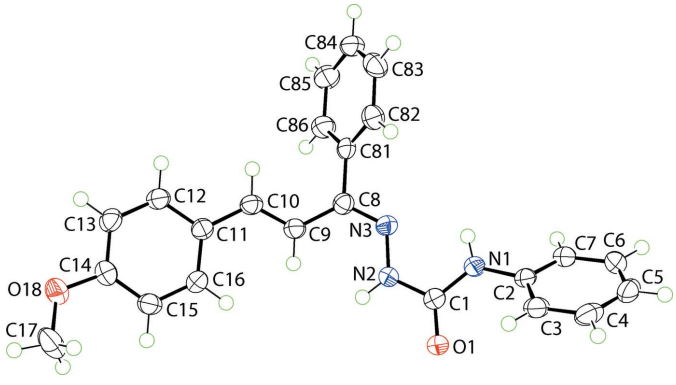

Figure 1
The molecular structure of (I), showing the atom-labelling scheme and displacement ellipsoids at the 70% probability level.

3. Supramolecular features

The most notable feature of the molecular packing of (I) is the presence of a centrosymmetric, eight-membered amide synthon, $\{\cdots OCNH\}_2$, Table 1. The resultant dimeric aggregate also incorporates two additional ethylene-C—H···O(amide) interactions, Fig. 2*a*, as well as methoxy-C—H···π(amine-phenyl) contacts, Table 1. The aggregates are assembled into a three-dimensional network *via* amine-phenyl-C—H···π(imine-phenyl) and methoxy-benzene-C—H···π(amine-phenyl) interactions, Fig. 2*b*.

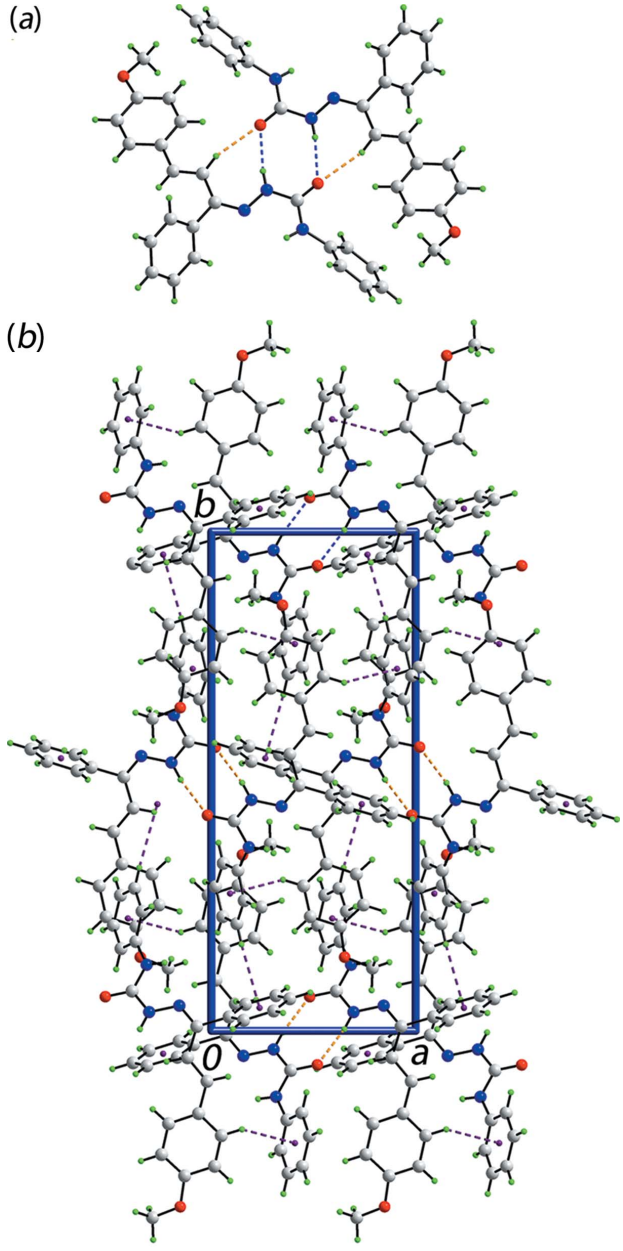

Figure 2
The molecular packing in (I): (*a*) a view of the supramolecular dimer sustained by amine-N—H···O(carbonyl) hydrogen bonds and supported by ethylene-C—H···O(amide) interactions, shown as blue and orange dashed lines, respectively, and (*b*) a view of the unit-cell contents shown in projection down the *c* axis. The C—H···π interactions are shown as purple dashed lines.

Table 1
Hydrogen-bond geometry (Å, °).

*Cg*1 and *Cg*2 are the centroids of the C2–C7 and C81–C86 rings, respectively.

D—H···*A*	*D*—H	H···*A*	*D*···*A*	*D*—H···*A*
N1—H1*N*···N3	0.87 (1)	2.18 (2)	2.6029 (15)	110 (1)
N2—H2*N*···O1^{i}	0.88 (1)	2.05 (1)	2.9184 (14)	171 (1)
C9—H9···O1^{i}	0.95	2.39	3.2913 (15)	159
C15—H15···*Cg*1^{i}	0.95	2.88	3.5125 (14)	125
C6—H6···*Cg*2^{ii}	0.95	2.92	3.8296 (14)	161
C12—H12···*Cg*1^{iii}	0.95	2.75	3.4715 (14)	133

Symmetry codes: (i) $-x+2, -y+1, -z+1$; (ii) $x-\frac{1}{2}, -y+\frac{1}{2}, z-\frac{1}{2}$; (iii) $-x+1, -y+1, -z+1$.

4. Analysis of the Hirshfeld surface

The Hirshfeld surface was calculated for (I) in accord with a recent report on a related molecule (Tan *et al.*, 2017) to provide more detailed information on the relative significance of the various intermolecular interactions. The donors and acceptors of intermolecular N—H···O and C—H···O interactions in (I) are viewed as the bright-red spots near the ethylene-H9, amide-H2*N* and carbonyl-O1 atoms on the Hirshfeld surface mapped over d_{norm} in Fig. 3*a*. The appearance of diminutive red spots near the N3 and C17 atoms, Fig. 3*a*, and the tiny faint-red spots near the C9 and H82 atoms in Fig. 3*b*, indicate the influence of short interatomic N3···C17 and C9···H82 contacts, Table 2. The donors and acceptors of intermolecular hydrogen bonds also appear as blue and red regions, respectively, around the participating atoms on the Hirshfeld surface mapped over the calculated electrostatic potential in Fig. 4. The involvement of the imine-phenyl (C81–C86) and amine-phenyl (C2–C7) rings as acceptors for C—H···π interactions are also evident through the light-red regions around these rings on the Hirshfeld surfaces in the views of Fig. 4. Referring to Fig. 5*a*, the concave region around the imine-phenyl ring on one side and the biconcave region around the amine-phenyl ring indicate their involvement in one and two C—H···π contacts, respectively. The short interatomic O···H/H···O contacts (Table 3) as well as N—H···O and C—H···O interactions about a reference molecule within shape-index mapped Hirshfeld surface, and the H···H, C···H/H···C and C···N/N···C contacts within the d_{norm}-mapped Hirshfeld surface are shown in Fig. 5*b* and *c*, respectively.

Table 2
Summary of short interatomic contacts (Å) in (I).

Contact	Distance	Symmetry operation
C17···N3	3.1147 (18)	$\frac{3}{2}-x, -\frac{1}{2}+y, \frac{1}{2}-z$
C9···H82	2.72	$1-x, 1-y, 1-z$
H86···H86	2.26	$1-x, 1-y, -z$
H12···H17*C*	2.26	$-\frac{1}{2}+x, \frac{1}{2}-y, -\frac{1}{2}+z$
O1···H16	2.61	$2-x, 1-y, 1-z$
O18···H84	2.67	$\frac{1}{2}-x, -\frac{1}{2}+y, \frac{1}{2}-z$
C8···H82	2.87	$1-x, 1-y, 1-z$
C12···H17*C*	2.79	$-\frac{1}{2}+x, \frac{1}{2}-y, -\frac{1}{2}+z$

Table 3
Percentage contributions of interatomic contacts to the Hirshfeld surface for (I).

Contact	Percentage contribution
H···H	50.2
C···H/H···C	31.6
O···H/H···O	10.7
N···H/H···N	4.2
N···O /O···N	0.9
C···O/O···C	0.9
C···C	0.8
C···N/N···C	0.7

The overall two dimensional fingerprint plot, Fig. 6*a*, and those delineated into H···H, C···H/H···C, O···H/H···O and N···H/H···N contacts (McKinnon *et al.*, 2007) are illustrated in Fig. 6*b*–*e*, respectively; the relative contributions from different interatomic contacts to the Hirshfeld surfaces are summarized in Table 3. The presence of a small but, distinctive peak at $d_e + d_i \sim 2.3$ Å in the fingerprint plot delineated into H···H contacts, and highlighted by a red arrow in Fig. 6*b*, results from the short interatomic H···H contact between symmetry-related imine-phenyl-H86 atoms, Table 2, whereas the flanking peaks, at the same $d_e + d_i \sim 2.3$ Å distance correspond to short interatomic H···H contacts between methoxybenzene-H12 and methoxy-H17*C* atoms, Table 2.

The C···H/H···C contacts in the crystal make the second largest contribution, *i.e.* 31.6%, to the Hirshfeld surface of (I), Fig. 6*c*, which is due to the presence of a significant number of C—H···π interactions involving the imine- and amine-phenyl rings, as well as short interatomic C···H/H···C contacts, Table 3, between the atoms of the methoxy-phenyl and imine-phenyl rings, Fig. 5*c*. The pair of forceps-like long tips at

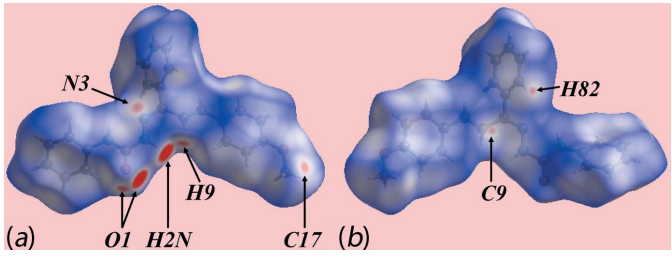

Figure 3
Two views of the Hirshfeld surface for (I) mapped over d_{norm} in the ranges (*a*) −0.225 to +1.332 a.u. and (*b*) −0.110 to +1.332 a.u.

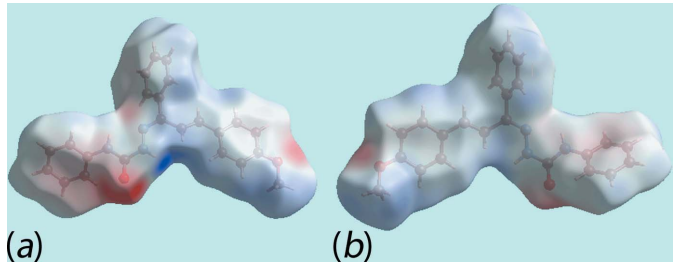

Figure 4
Two views of the Hirshfeld surface for (I) mapped over the electrostatic potential in the range −0.095 to +0.108 a.u. The red and blue regions represent negative and positive electrostatic potentials, respectively.

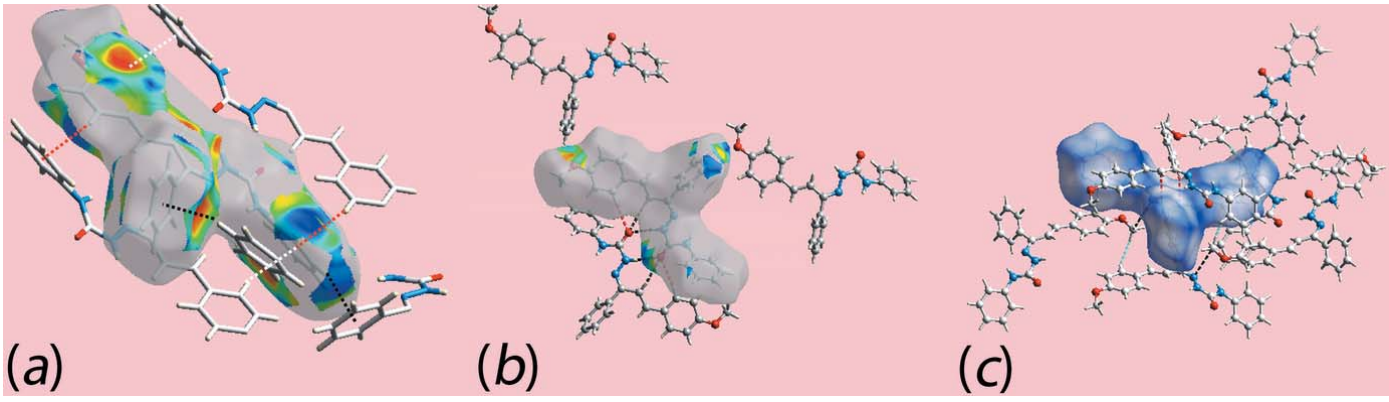

Figure 5
Views of the Hirshfeld surfaces about a reference molecule mapped over (*a*) the shape-index property showing C—H···π/π···H—C interactions involving the C6 atom with the imine–phenyl C81–C86 ring (black dotted lines) and the C12 and C15 atoms with the amine–phenyl C2–C7 rings by red and white dotted lines, respectively, (*b*) the shape-index property about a reference molecule showing short O···H/H···O contacts by red dotted lines and intermolecular N—H···O and C—H···O interactions by black dashed lines and (*c*) d_{norm} showing short interatomic H···H, C···N/N···C and C···H/H···C contacts by sky-blue, black and red dashed lines, respectively.

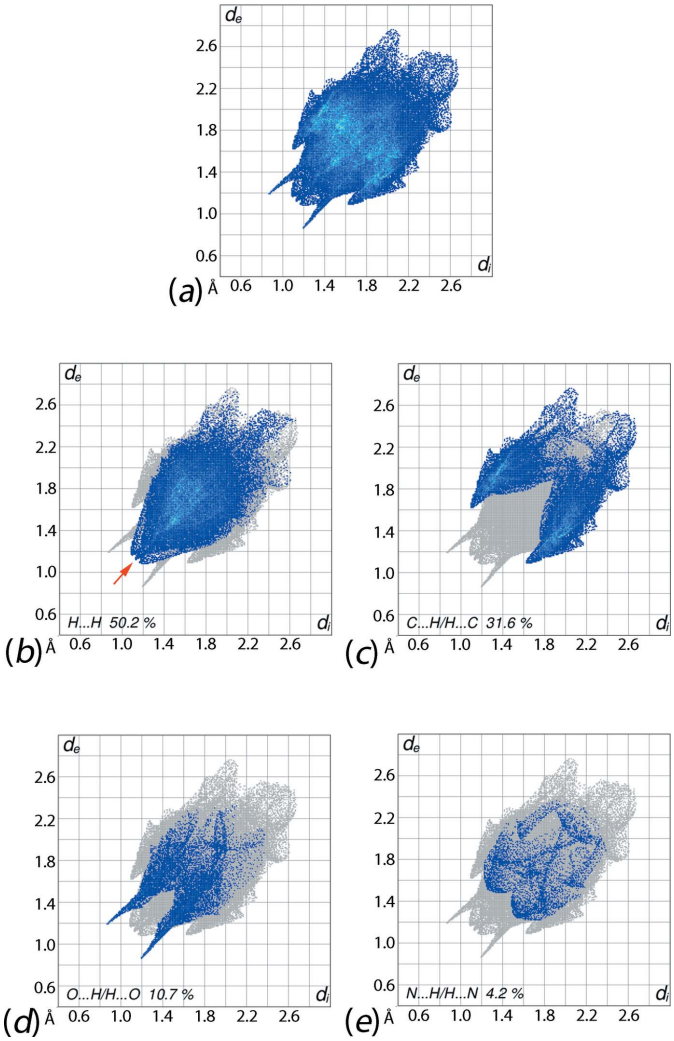

Figure 6
(*a*) The full two-dimensional fingerprint plot for (I) and those delineated into (*b*) H···H, (*c*) C···H/H···C, (*d*) O···H/H···O and (*e*) N···H/H···N contacts.

$d_e + d_i$ = 2.1 Å in the fingerprint plot delineated into O···H/H···O contacts, Fig. 6*d*, reflect the presence the N—H···O hydrogen bond; the pair of spikes corresponding to the C—H···O contacts and the points related to short interatomic O···H/H···O contacts, Table 2, are merged within the plot. Although the N···H/H···N contacts have a notable contribution of 4.2% to the Hirshfeld surface, Fig. 6*e*, as their interatomic distances are greater than their van der Waals separations, they do not make a specific contribution to the molecular packing. The participation of the methyl-C17 atom in two close interatomic contacts, Table 2, brings into close proximity the methyl-C17 and imine-N3 atoms, Table 2, but these are interspersed by the H17*A* and H17*B* atoms so are not surface contacts. Finally, the small contributions from other interatomic contacts summarized in Table 3 have a negligible effect on the structure.

5. Database survey

The title compound was prepared from the dehydrogenation reaction of 4-phenylsemicarbazide and 4-methoxychalcone. A search of the Cambridge Structural Database (Groom *et al.*, 2016) revealed no direct precedents for this type of molecule. The most closely related structure is one where the ethylene bond is incorporated within a five-membered pyrazolone ring (Chai *et al.*, 2005). Here, the intramolecular amine-N—H···N(imine) hydrogen bond persists in each of the two independent molecules comprising the asymmetric unit, as do the *E*-conformations about the two analogous double bonds in the molecule. However, there is considerable twisting about the equivalent bonds to C8—C9 in (I), *i.e.* the N—C—C—C torsion angles are 130.3 (6) and 136.0 (6)°, *cf.* 154.62 (12)° in (I), an observation attributed to the need to reduce steric hindrance between the rings in the molecules.

Table 4
Experimental details.

Crystal data	
Chemical formula	$C_{23}H_{21}N_3O_2$
M_r	371.43
Crystal system, space group	Monoclinic, $P2_1/n$
Temperature (K)	100
a, b, c (Å)	9.2879 (2), 21.9137 (3), 9.6740 (2)
β (°)	105.187 (2)
V (Å^3)	1900.21 (6)
Z	4
Radiation type	Cu $K\alpha$
μ (mm^{-1})	0.68
Crystal size (mm)	0.31 × 0.29 × 0.16
Data collection	
Diffractometer	Oxford Diffraction Xcaliber Eos Gemini
Absorption correction	Multi-scan (*CrysAlis PRO*; Agilent, 2011)
T_{min}, T_{max}	0.904, 1.000
No. of measured, independent and observed [$I > 2\sigma(I)$] reflections	25449, 3678, 3380
R_{int}	0.025
(sin $\theta/\lambda)_{max}$ (Å^{-1})	0.615
Refinement	
$R[F^2 > 2\sigma(F^2)]$, $wR(F^2)$, S	0.038, 0.104, 1.03
No. of reflections	3678
No. of parameters	260
No. of restraints	2
H-atom treatment	H atoms treated by a mixture of independent and constrained refinement
$\Delta\rho_{max}$, $\Delta\rho_{min}$ (e Å^{-3})	0.22, −0.24

Computer programs: *CrysAlis PRO* (Agilent, 2011), *SHELXS* (Sheldrick, 2008), *SHELXL2014/7* (Sheldrick, 2015), *ORTEP-3 for Windows* (Farrugia, 2012), *DIAMOND* (Brandenburg, 2006) and *publCIF* (Westrip, 2010).

6. Synthesis and crystallization

Analytical grade reagents were used as procured without further purification. 4-Phenylsemicarbazide (1.51 g, 0.01 mol) and 4-methoxychalcone (2.38 g, 0.01 mol) were dissolved separately in hot absolute ethanol (30 ml) and mixed with stirring. A few drops of concentrated hydrochloric acid were added as a catalyst. The reaction mixture was heated and stirred for about 20 min., then stirred for a further 30 min. at room temperature. The resulting yellow precipitate was filtered, washed with cold ethanol and dried *in vacuo*; yield: 75%. Single crystals were grown at room temperature from the slow evaporation of mixed ethanol and acetonitrile solvents (1:1 *v*/*v*; 20 ml), m.p. 407 K. IR (cm^{-1}): 3336 ν(N—H), 1679 ν(C=O), 1526 ν(C=N), 1242 ν(C—N), 1025 ν(C=S). MS (*m*/*z*): 371.25 $[M+1]^+$.

7. Refinement

Crystal data, data collection and structure refinement details are summarized in Table 4. The carbon-bound H atoms were placed in calculated positions (C—H = 0.95–0.98 Å) and were included in the refinement in the riding-model approximation, with U_{iso}(H) set to 1.2–1.5U_{eq}(C). The nitrogen-bound H atoms were located in a difference-Fourier map but were refined with a distance restraint of N—H = 0.88±0.01 Å, and with U_{iso}(H) set to 1.2U_{eq}(N).

Acknowledgements

We thank the staff of the University of Malaya's X-ray diffraction laboratory for the data collection.

Funding information

The authors are grateful for support from the Universiti Putra Malaysia, under their Research University Grant Scheme (RUGS Nos 9199834 and 9174000) and to the Malaysian Ministry of Science, Technology and Innovation (grants No. 09–02-04–0752-EA001 and 01-01-16-1833FR).

References

Agilent (2011). *CrysAlis PRO*. Agilent Technologies, Yarnton, England.
Brandenburg, K. (2006). *DIAMOND*. Crystal Impact GbR, Bonn, Germany.
Chai, H., Liu, G., Liu, L., Jia, D., Guo, Z. & Lang, J. (2005). *J. Mol. Struct.* **752**, 124–129.
Farrugia, L. J. (2012). *J. Appl. Cryst.* **45**, 849–854.
Gaonkar, S. L. & Vignesh, U. N. (2017). *Res .Chem. Intermed*. https://doi. org/10.1007/s11164-017-2977-5.
Groom, C. R., Bruno, I. J., Lightfoot, M. P. & Ward, S. C. (2016). *Acta Cryst.* B**72**, 171–179.
Kumar, A., Gupta, V., Singh, S. & Gupta, Y. (2017). *Asia. J. Rese. Chem.* **10**, 225–239.
Li, J., Li, D., Xu, Y., Guo, Z., Liu, X., Yang, H., Wu, L. & Wang, L. (2017). *Bioorg. Med. Chem. Lett.* **27**, 602–606.
Mahapatra, D. K., Bharti, S. K. & Asati, V. (2015). *Eur. J. Med. Chem.* **98**, 69–114.
McKinnon, J. J., Jayatilaka, D. & Spackman, M. A. (2007). *Chem. Commun.* pp. 3814–3816.
Sharma, C., Verma, T., Singh, H. & Kumar, N. (2014). *Med. Chem. Res.* **23**, 4814–4824.
Sheldrick, G. M. (2008). *Acta Cryst.* A**64**, 112–122.
Sheldrick, G. M. (2015). *Acta Cryst.* C**71**, 3–8.
Singh, H. P., Singhal, M., Chauhan, C., Pandey, S., Paul, A. & Sharma, Y. C. S. (2010). *Pharmacologyonline*, **1**, 448–458.
Singhal, M., Paul, A., Tiwari, A. K. & Songara, R. K. (2011). *Res. Rev. BioSciences*, **5**, 131–133.
Syahri, J., Rullah, K., Armunanto, R., Yuanita, E., Nurohmah, B. A., Mohd Aluwi, M. F. F., Wai, L. K. & Purwono, B. (2017). *Asia. Pac. J. Trop. Dis.* **7**, 8–13.
Tan, M. Y., Crouse, K. A., Ravoof, T. B. S. A., Jotani, M. M. & Tiekink, E. R. T. (2017). *Acta Cryst.* E**73**, 1001–1008.
Tan, M. Y., Crouse, K. A., Ravoof, T. B. S. A. & Tiekink, E. R. T. (2015). *Acta Cryst.* E**71**, o1047–o1048.
Westrip, S. P. (2010). *J. Appl. Cryst.* **43**, 920–925.
Xie, Z., Luo, X., Zou, Z., Zhang, X., Huang, F., Li, R., Liao, S. & Liu, Y. (2017). *Bioorg. Med. Chem. Lett.* **27**, 3602–3606.
Zhuang, C., Zhang, W., Sheng, C., Zhang, W., Xing, C. & Miao, Z. (2017). *Chem. Rev.* **117**, 7762–7810.

supporting information

Acta Cryst. (2017). E**73**, 1607-1611 [https://doi.org/10.1107/S2056989017014128]

1-{(*E*)-[(2*E*)-3-(4-Methoxyphenyl)-1-phenylprop-2-en-1-ylidene]amino}-3-phenylurea: crystal structure and Hirshfeld surface analysis

Ming Yueh Tan, Karen A. Crouse, Thahira B. S. A. Ravoof, Mukesh M. Jotani and Edward R. T. Tiekink

Computing details

Data collection: *CrysAlis PRO* (Agilent, 2011); cell refinement: *CrysAlis PRO* (Agilent, 2011); data reduction: *CrysAlis PRO* (Agilent, 2011); program(s) used to solve structure: *SHELXS* (Sheldrick, 2008); program(s) used to refine structure: *SHELXL2014/7* (Sheldrick, 2015); molecular graphics: *ORTEP-3 for Windows* (Farrugia, 2012) and *DIAMOND* (Brandenburg, 2006); software used to prepare material for publication: *publCIF* (Westrip, 2010).

1-{(*E*)-[(2*E*)-3-(4-Methoxyphenyl)-1-phenylprop-2-en-1-ylidene]amino}-3-phenylurea

Crystal data

$C_{23}H_{21}N_3O_2$
$M_r = 371.43$
Monoclinic, $P2_1/n$
$a = 9.2879$ (2) Å
$b = 21.9137$ (3) Å
$c = 9.6740$ (2) Å
$\beta = 105.187$ (2)°
$V = 1900.21$ (6) Å^3
$Z = 4$
$F(000) = 784$
$D_x = 1.298$ Mg m^{-3}
Cu $K\alpha$ radiation, $\lambda = 1.5418$ Å
Cell parameters from 12038 reflections
$\theta = 4.0$–$71.3°$
$\mu = 0.68$ mm^{-1}
$T = 100$ K
Slab (cut), light-yellow
0.31 × 0.29 × 0.16 mm

Data collection

Oxford Diffraction Xcaliber Eos Gemini diffractometer
Radiation source: fine-focus sealed tube
Graphite monochromator
Detector resolution: 16.1952 pixels mm^{-1}
ω scans
Absorption correction: multi-scan (CrysAlis PRO; Agilent, 2011)
$T_{min} = 0.904$, $T_{max} = 1.000$
25449 measured reflections
3678 independent reflections
3380 reflections with $I > 2\sigma(I)$
$R_{int} = 0.025$
$\theta_{max} = 71.4°$, $\theta_{min} = 4.0°$
$h = -11 \rightarrow 11$
$k = -26 \rightarrow 26$
$l = -11 \rightarrow 11$

Refinement

Refinement on F^2
Least-squares matrix: full
$R[F^2 > 2\sigma(F^2)] = 0.038$
$wR(F^2) = 0.104$
$S = 1.03$
3678 reflections
260 parameters
2 restraints
Primary atom site location: structure-invariant direct methods
Hydrogen site location: mixed
H atoms treated by a mixture of independent and constrained refinement
$w = 1/[\sigma^2(F_o^2) + (0.0583P)^2 + 0.6586P]$ where $P = (F_o^2 + 2F_c^2)/3$
$(\Delta/\sigma)_{max} = 0.001$

$\Delta\rho_{max}$ = 0.22 e Å^{-3} $\Delta\rho_{min}$ = −0.24 e Å^{-3}

Special details

Geometry. All esds (except the esd in the dihedral angle between two l.s. planes) are estimated using the full covariance matrix. The cell esds are taken into account individually in the estimation of esds in distances, angles and torsion angles; correlations between esds in cell parameters are only used when they are defined by crystal symmetry. An approximate (isotropic) treatment of cell esds is used for estimating esds involving l.s. planes.

Fractional atomic coordinates and isotropic or equivalent isotropic displacement parameters (Å^2)

	x	*y*	*z*	U_{iso}*/U_{eq}
O1	1.01879 (9)	0.56831 (4)	0.59686 (10)	0.0282 (2)
O18	0.65222 (10)	0.14747 (4)	0.28503 (10)	0.0303 (2)
N1	0.81663 (12)	0.63230 (5)	0.54527 (11)	0.0253 (2)
H1N	0.7293 (12)	0.6365 (7)	0.4858 (14)	0.030*
N2	0.80445 (11)	0.53742 (5)	0.44127 (11)	0.0230 (2)
H2N	0.8494 (16)	0.5033 (5)	0.4302 (16)	0.028*
N3	0.65679 (11)	0.55029 (5)	0.37877 (11)	0.0224 (2)
C1	0.88811 (13)	0.57941 (6)	0.53281 (13)	0.0227 (3)
C2	0.86973 (13)	0.67870 (6)	0.64749 (13)	0.0234 (3)
C3	0.94222 (14)	0.66456 (6)	0.78919 (14)	0.0267 (3)
H3	0.9657	0.6234	0.8168	0.032*
C4	0.97992 (14)	0.71113 (7)	0.88961 (14)	0.0314 (3)
H4	1.0300	0.7017	0.9861	0.038*
C5	0.94507 (14)	0.77139 (7)	0.85028 (15)	0.0337 (3)
H5	0.9688	0.8029	0.9200	0.040*
C6	0.87558 (14)	0.78537 (6)	0.70894 (16)	0.0312 (3)
H6	0.8527	0.8266	0.6816	0.037*
C7	0.83916 (13)	0.73922 (6)	0.60681 (14)	0.0263 (3)
H7	0.7935	0.7490	0.5095	0.032*
C8	0.57139 (13)	0.50863 (5)	0.30443 (12)	0.0215 (3)
C9	0.61677 (13)	0.44598 (6)	0.28545 (13)	0.0221 (3)
H9	0.7195	0.4382	0.2945	0.026*
C10	0.52152 (13)	0.39879 (6)	0.25590 (12)	0.0223 (3)
H10	0.4180	0.4081	0.2305	0.027*
C11	0.56261 (13)	0.33419 (6)	0.25920 (12)	0.0216 (3)
C12	0.45125 (13)	0.28994 (6)	0.21358 (13)	0.0239 (3)
H12	0.3505	0.3026	0.1776	0.029*
C13	0.48453 (14)	0.22853 (6)	0.21976 (13)	0.0253 (3)
H13	0.4078	0.1994	0.1850	0.030*
C14	0.63070 (14)	0.20925 (6)	0.27707 (13)	0.0232 (3)
C15	0.74391 (14)	0.25212 (6)	0.32357 (13)	0.0253 (3)
H15	0.8441	0.2392	0.3619	0.030*
C16	0.70944 (14)	0.31380 (6)	0.31361 (13)	0.0247 (3)
H16	0.7872	0.3429	0.3444	0.030*
C17	0.78852 (18)	0.12581 (7)	0.37548 (15)	0.0384 (4)
H17A	0.8711	0.1373	0.3351	0.058*
H17B	0.7845	0.0813	0.3829	0.058*
H17C	0.8041	0.1439	0.4709	0.058*

C81	0.41306 (13)	0.52769 (5)	0.24448 (13)	0.0222 (3)
C82	0.33269 (14)	0.55311 (6)	0.33371 (14)	0.0259 (3)
H82	0.3795	0.5587	0.4327	0.031*
C83	0.18453 (15)	0.57034 (6)	0.27873 (15)	0.0299 (3)
H83	0.1298	0.5865	0.3408	0.036*
C84	0.11639 (14)	0.56408 (6)	0.13362 (16)	0.0314 (3)
H84	0.0157	0.5765	0.0960	0.038*
C85	0.19547 (15)	0.53967 (7)	0.04391 (15)	0.0345 (3)
H85	0.1494	0.5357	−0.0557	0.041*
C86	0.34221 (15)	0.52092 (6)	0.09928 (14)	0.0298 (3)
H86	0.3950	0.5033	0.0374	0.036*

Atomic displacement parameters (Å²)

	U^{11}	U^{22}	U^{33}	U^{12}	U^{13}	U^{23}
O1	0.0186 (4)	0.0265 (5)	0.0361 (5)	0.0021 (3)	0.0011 (4)	−0.0090 (4)
O18	0.0325 (5)	0.0216 (5)	0.0364 (5)	0.0031 (4)	0.0085 (4)	0.0038 (4)
N1	0.0203 (5)	0.0252 (5)	0.0256 (5)	0.0034 (4)	−0.0024 (4)	−0.0063 (4)
N2	0.0192 (5)	0.0194 (5)	0.0281 (5)	0.0018 (4)	0.0019 (4)	−0.0027 (4)
N3	0.0190 (5)	0.0224 (5)	0.0239 (5)	0.0002 (4)	0.0022 (4)	0.0004 (4)
C1	0.0200 (6)	0.0234 (6)	0.0241 (6)	−0.0006 (5)	0.0047 (5)	−0.0016 (5)
C2	0.0157 (5)	0.0270 (6)	0.0266 (6)	0.0003 (5)	0.0039 (5)	−0.0074 (5)
C3	0.0189 (6)	0.0330 (7)	0.0274 (6)	0.0020 (5)	0.0045 (5)	−0.0030 (5)
C4	0.0196 (6)	0.0488 (8)	0.0244 (6)	−0.0017 (6)	0.0035 (5)	−0.0097 (6)
C5	0.0218 (6)	0.0415 (8)	0.0379 (7)	−0.0047 (6)	0.0082 (5)	−0.0211 (6)
C6	0.0224 (6)	0.0273 (7)	0.0444 (8)	0.0006 (5)	0.0099 (6)	−0.0113 (6)
C7	0.0194 (6)	0.0286 (7)	0.0291 (6)	0.0025 (5)	0.0034 (5)	−0.0050 (5)
C8	0.0219 (6)	0.0215 (6)	0.0207 (6)	−0.0009 (5)	0.0046 (4)	0.0003 (4)
C9	0.0192 (6)	0.0236 (6)	0.0223 (6)	0.0013 (5)	0.0034 (4)	−0.0008 (4)
C10	0.0185 (6)	0.0254 (6)	0.0213 (6)	0.0010 (5)	0.0023 (4)	0.0000 (5)
C11	0.0212 (6)	0.0231 (6)	0.0200 (6)	−0.0004 (5)	0.0047 (4)	−0.0001 (4)
C12	0.0195 (6)	0.0256 (6)	0.0257 (6)	−0.0001 (5)	0.0044 (5)	0.0031 (5)
C13	0.0236 (6)	0.0237 (6)	0.0284 (6)	−0.0044 (5)	0.0066 (5)	0.0020 (5)
C14	0.0290 (6)	0.0210 (6)	0.0214 (6)	0.0016 (5)	0.0096 (5)	0.0022 (4)
C15	0.0214 (6)	0.0278 (6)	0.0256 (6)	0.0040 (5)	0.0041 (5)	−0.0014 (5)
C16	0.0211 (6)	0.0240 (6)	0.0278 (6)	−0.0024 (5)	0.0042 (5)	−0.0038 (5)
C17	0.0510 (9)	0.0276 (7)	0.0311 (7)	0.0153 (6)	0.0012 (6)	−0.0011 (6)
C81	0.0214 (6)	0.0155 (5)	0.0283 (6)	−0.0018 (4)	0.0036 (5)	0.0007 (5)
C82	0.0294 (7)	0.0212 (6)	0.0270 (6)	0.0012 (5)	0.0073 (5)	0.0036 (5)
C83	0.0305 (7)	0.0228 (6)	0.0400 (7)	0.0032 (5)	0.0159 (6)	0.0043 (5)
C84	0.0200 (6)	0.0262 (6)	0.0448 (8)	0.0016 (5)	0.0028 (6)	0.0028 (6)
C85	0.0278 (7)	0.0371 (8)	0.0321 (7)	0.0023 (6)	−0.0034 (5)	−0.0046 (6)
C86	0.0250 (7)	0.0329 (7)	0.0294 (7)	0.0023 (5)	0.0035 (5)	−0.0056 (5)

Geometric parameters (Å, º)

O1—C1	1.2338 (15)	C10—H10	0.9500
O18—C14	1.3677 (15)	C11—C16	1.4002 (17)

O18—C17	1.4189 (17)	C11—C12	1.4020 (17)
N1—C1	1.3566 (16)	C12—C13	1.3787 (18)
N1—C2	1.4140 (16)	C12—H12	0.9500
N1—H1N	0.868 (9)	C13—C14	1.3909 (17)
N2—C1	1.3691 (16)	C13—H13	0.9500
N2—N3	1.3754 (14)	C14—C15	1.3937 (18)
N2—H2N	0.877 (9)	C15—C16	1.3865 (18)
N3—C8	1.2964 (16)	C15—H15	0.9500
C2—C7	1.3914 (18)	C16—H16	0.9500
C2—C3	1.3945 (18)	C17—H17A	0.9800
C3—C4	1.3891 (19)	C17—H17B	0.9800
C3—H3	0.9500	C17—H17C	0.9800
C4—C5	1.389 (2)	C81—C86	1.3943 (18)
C4—H4	0.9500	C81—C82	1.3964 (18)
C5—C6	1.385 (2)	C82—C83	1.3913 (19)
C5—H5	0.9500	C82—H82	0.9500
C6—C7	1.3923 (18)	C83—C84	1.387 (2)
C6—H6	0.9500	C83—H83	0.9500
C7—H7	0.9500	C84—C85	1.383 (2)
C8—C9	1.4616 (17)	C84—H84	0.9500
C8—C81	1.4922 (17)	C85—C86	1.3896 (19)
C9—C10	1.3422 (17)	C85—H85	0.9500
C9—H9	0.9500	C86—H86	0.9500
C10—C11	1.4643 (17)		

C14—O18—C17	117.36 (10)	C12—C11—C10	119.68 (11)
C1—N1—C2	125.97 (10)	C13—C12—C11	121.53 (11)
C1—N1—H1N	115.3 (11)	C13—C12—H12	119.2
C2—N1—H1N	118.7 (11)	C11—C12—H12	119.2
C1—N2—N3	118.57 (10)	C12—C13—C14	119.87 (11)
C1—N2—H2N	116.4 (10)	C12—C13—H13	120.1
N3—N2—H2N	125.0 (10)	C14—C13—H13	120.1
C8—N3—N2	119.61 (10)	O18—C14—C13	115.85 (11)
O1—C1—N1	124.31 (11)	O18—C14—C15	124.21 (11)
O1—C1—N2	120.62 (11)	C13—C14—C15	119.94 (11)
N1—C1—N2	115.07 (10)	C16—C15—C14	119.58 (11)
C7—C2—C3	120.00 (12)	C16—C15—H15	120.2
C7—C2—N1	118.66 (11)	C14—C15—H15	120.2
C3—C2—N1	121.19 (12)	C15—C16—C11	121.45 (12)
C4—C3—C2	119.51 (13)	C15—C16—H16	119.3
C4—C3—H3	120.2	C11—C16—H16	119.3
C2—C3—H3	120.2	O18—C17—H17A	109.5
C5—C4—C3	120.59 (13)	O18—C17—H17B	109.5
C5—C4—H4	119.7	H17A—C17—H17B	109.5
C3—C4—H4	119.7	O18—C17—H17C	109.5
C6—C5—C4	119.72 (12)	H17A—C17—H17C	109.5
C6—C5—H5	120.1	H17B—C17—H17C	109.5
C4—C5—H5	120.1	C86—C81—C82	118.53 (11)

C5—C6—C7	120.25 (13)	C86—C81—C8	121.24 (11)
C5—C6—H6	119.9	C82—C81—C8	120.23 (11)
C7—C6—H6	119.9	C83—C82—C81	120.48 (12)
C2—C7—C6	119.87 (12)	C83—C82—H82	119.8
C2—C7—H7	120.1	C81—C82—H82	119.8
C6—C7—H7	120.1	C84—C83—C82	120.22 (12)
N3—C8—C9	125.20 (11)	C84—C83—H83	119.9
N3—C8—C81	114.57 (11)	C82—C83—H83	119.9
C9—C8—C81	120.09 (10)	C85—C84—C83	119.78 (12)
C10—C9—C8	123.70 (11)	C85—C84—H84	120.1
C10—C9—H9	118.2	C83—C84—H84	120.1
C8—C9—H9	118.2	C84—C85—C86	120.07 (13)
C9—C10—C11	125.93 (11)	C84—C85—H85	120.0
C9—C10—H10	117.0	C86—C85—H85	120.0
C11—C10—H10	117.0	C85—C86—C81	120.88 (13)
C16—C11—C12	117.59 (11)	C85—C86—H86	119.6
C16—C11—C10	122.64 (11)	C81—C86—H86	119.6

C1—N2—N3—C8	−172.44 (11)	C10—C11—C12—C13	−177.65 (11)
C2—N1—C1—O1	−10.4 (2)	C11—C12—C13—C14	2.34 (19)
C2—N1—C1—N2	169.88 (12)	C17—O18—C14—C13	−163.67 (12)
N3—N2—C1—O1	176.21 (11)	C17—O18—C14—C15	15.55 (17)
N3—N2—C1—N1	−4.07 (16)	C12—C13—C14—O18	177.07 (11)
C1—N1—C2—C7	144.18 (13)	C12—C13—C14—C15	−2.19 (18)
C1—N1—C2—C3	−40.29 (19)	O18—C14—C15—C16	−178.53 (11)
C7—C2—C3—C4	1.68 (19)	C13—C14—C15—C16	0.66 (18)
N1—C2—C3—C4	−173.79 (11)	C14—C15—C16—C11	0.76 (19)
C2—C3—C4—C5	0.48 (19)	C12—C11—C16—C15	−0.63 (18)
C3—C4—C5—C6	−1.7 (2)	C10—C11—C16—C15	175.98 (12)
C4—C5—C6—C7	0.7 (2)	N3—C8—C81—C86	127.82 (13)
C3—C2—C7—C6	−2.62 (19)	C9—C8—C81—C86	−56.24 (16)
N1—C2—C7—C6	172.96 (11)	N3—C8—C81—C82	−51.92 (16)
C5—C6—C7—C2	1.42 (19)	C9—C8—C81—C82	124.02 (12)
N2—N3—C8—C9	3.18 (18)	C86—C81—C82—C83	0.97 (18)
N2—N3—C8—C81	178.88 (10)	C8—C81—C82—C83	−179.28 (11)
N3—C8—C9—C10	154.62 (12)	C81—C82—C83—C84	−1.90 (19)
C81—C8—C9—C10	−20.85 (18)	C82—C83—C84—C85	1.1 (2)
C8—C9—C10—C11	−169.19 (11)	C83—C84—C85—C86	0.6 (2)
C9—C10—C11—C16	9.05 (19)	C84—C85—C86—C81	−1.6 (2)
C9—C10—C11—C12	−174.41 (12)	C82—C81—C86—C85	0.76 (19)
C16—C11—C12—C13	−0.93 (18)	C8—C81—C86—C85	−178.98 (12)

Hydrogen-bond geometry (Å, º)

*Cg*1 and *Cg*2 are the centroids of the C2–C7 and C81–C86 rings, respectively.

D—H···*A*	*D*—H	H···*A*	*D*···*A*	*D*—H···*A*
N1—H1*N*···N3	0.87 (1)	2.18 (2)	2.6029 (15)	110 (1)
N2—H2*N*···O1^{i}	0.88 (1)	2.05 (1)	2.9184 (14)	171 (1)

C9—H9···O1^{i}	0.95	2.39	3.2913 (15)	159
C15—H15···*Cg*1^{i}	0.95	2.88	3.5125 (14)	125
C6—H6···*Cg*2^{ii}	0.95	2.92	3.8296 (14)	161
C12—H12···*Cg*1^{iii}	0.95	2.75	3.4715 (14)	133

Symmetry codes: (i) −*x*+2, −*y*+1, −*z*+1; (ii) *x*−1/2, −*y*+1/2, *z*−1/2; (iii) −*x*+1, −*y*+1, −*z*+1.